where

$$z = \ell_n\{1 - \varepsilon \cos \tilde{\beta}\sqrt{(a_0/\mu)}t\} \qquad (13b)$$

It is found that Eq. (13a) may then be integrated by parts to yield

$$\Omega(t) = \Omega_0 + \frac{3}{2}\frac{J_2}{(\varepsilon/g_0)\cos\tilde{\beta}}\left\{\frac{R}{a_0}\right\}^2 \{\exp\{8z\}[8\cos(mz+i_0)$$

$$+ m\sin(mz+i_0)] - [8\cos(i_0) + m\sin(i_0)]\} \qquad (14a)$$

where

$$m = -(2/\pi)\tan\tilde{\beta} \qquad (14b)$$

A set of closed-form solutions representing the evolution of an expanding, precessing quasicircular orbit with continuous plane change have now been obtained. These solutions will now be used in an illustrative example.

IV. Example: Low-Thrust Spiral

To illustrate the use of the solutions, a simple spiral maneuver will be investigated. A low-thrust vehicle with an acceleration ε of 1 mm s^{-2} will be considered with an initial altitude of 400 km and an inclination of 89.5 deg. The Edelbaum steering law will be used with $\tilde{\beta} = 10$ deg to increase the orbital inclination as the vehicle sprials outward.

The change in elements is shown in Fig. 2 over a period of 50 days. Numerical solutions obtained from the full nonlinear dynamics are also shown for comparison. It can be seen that the nodal rate changes sign as the vehicle orbit becomes retrograde. In addition, the increase in ascending node slows as the vehicle altitude increases. This is due to the strong coupling of nodal rate to semimajor axis. The total change in ascending node angle is seen to be small due to the high initial inclination. However, for lower inclinations substantial changes in ascending node angle can accumulate.[9] It can be seen that the analytic solutions prove accurate and capture coupling effects in the dynamics such as nodal rate reversals.

V. Conclusions

The dynamics of a low-thrust orbital transfer vehicle under the action of Earth-oblateness perturbations has been considered. A set of coupled, orbit-averaged equations have been derived, which may be solved sequentially. Analytic solutions for semimajor axis, true anomaly, inclination, and ascending node angle have been obtained. These solutions extend previous, well-known solutions for low-thrust spiral motion and may be used for mission analysis and design purposes.

References

[1]Wakker, K. E., *Rocket Propulsion and Spaceflight Dynamics*, Pitman, London, 1984, pp. 462–479.

[2]Wiesel, W. E., *Spaceflight Dynamics*, McGraw–Hill, New York, 1991, pp. 89–91.

[3]Edelbaum, T. E., "Propulsion Requirements for Controllable Satellites," *American Rocket Society Journal*, Vol. 31, No. 8, 1961, pp. 1079–1089.

[4]Wiesel, W. E., and Alfano, S., "Optimal Many-Revolution Orbit Transfer," *Journal of Guidance, Control, and Dynamics*, Vol. 8, No. 1, 1985, pp. 155–157.

[5]Martin, A. R., and Cresdee, M. T., "The Use of Electric Propulsion for Low Earth Orbit Spacecraft," *Journal of the British Interplanetary Society*, Vol. 41, June 1988, pp. 175–182.

[6]Deininger, W. D., and Vondra, R. J., "Electric Propulsion for Constellation Deployment and Spacecraft Maneuvering," *Journal of Spacecraft and Rockets*, Vol. 26, No. 5, 1989, pp. 352–357.

[7]Welch, C. S., "Servicing Polar Platforms Using Low-Thrust Propulsion," 44th International Astronautical Federation Congress, IAF-93-A.6.54, Graz, Austria, Oct. 1993.

[8]Roy, A. E., *Orbital Motion*, Adam Hilger, Bristol, England, UK, 1992, pp. 183–186.

[9]McInnes, C. R., "Low-Thrust Orbit Raising with J_2 Precession," Dept. of Aerospace Engineering, Rept. 9608, Univ. of Glasgow, Scotland, UK, May 1996.

Path Planning for Space Manipulators to Reduce Attitude Disturbances

Hiroshi Okubo,* Nobuo Nagano,† Nobuo Komatsu,‡ and Toshihiro Tsumura§
Osaka Prefecture University, Sakai, Osaka 593, Japan

Introduction

FOR future activities in space, the role of robotic manipulators carried by a spacecraft will be important and it has received considerable attention. However, for practical applications, there will be many dynamic and control problems due to the dynamic coupling between the manipulator arm and the spacecraft main body. The attitude of the spacecraft will be disturbed by movement of a manipulator whereas steady-state condition is desirable for many reasons such as keeping communication links and using vision systems. A number of studies have analyzed the dynamic coupling problems and proposed methods of planning the path of space manipulators from the above point of view.[1,2] Dubowsky and his group developed an approach to the manipulator path planning that gives minimum disturbance to the spacecraft attitude.[3,4] This approach makes use of an aid called a disturbance map (DM) or enhanced disturbance map (EDM). They proposed a method for planning the minimum-disturbance manipulator path that gives the minimum fuel consumption for attitude control. This approach is most attractive for its simplicity although it assumes the use of the attitude control system for the spacecraft main body. Moreover, the applications are restricted to two- or three-link manipulators because the planning procedure requires joint space visualization and ad hoc decisions. This Note proposes a new method for planning the manipulator path using an algorithm based on the concept of EDM. The method sequentially determines the direction of joint movements in the joint space that simultaneously minimizes the disturbance to the spacecraft attitude and realizes the desired terminal joint angles.

EDM

We here consider a space robot system in two-dimensional space. When there are no external forces and torque, with zero initial angular momentum, the conservation of the angular momentum provides the relation between the spacecraft attitude variation $\delta\chi$ and the small angular movements of the manipulator joints $\delta\boldsymbol{q}$. This relation enables us to draw an EDM[4] for the method of path planning. The EDM shows the direction of joint movements, at each point in the joint space, that causes zero disturbance to the spacecraft attitude due to the manipulator motion as well as the magnitude of the maximum attitude disturbance. Figure 1 shows an example of EDM for a planner space robot with a two-link manipulator. The plotted lines are zero-disturbance lines along which attitude disturbance is zero, and the contour map shows magnitude of the maximum disturbance. The darker area of the contour map shows the higher magnitude of the maximum disturbance. The feature of the EDM varies depending on the specific mass and length parameters of the bodies in the system.

*Associate Professor, Department of Aerospace Engineering. Member AIAA.

†Graduate Student; currently Research Engineer, Sumitomo Precision Products Co., Ltd., Amagasaki 660, Japan.

‡Research Associate; currently Assistant Professor, Shizuoka Institute of Science and Technology, Fukuroi 437, Japan.

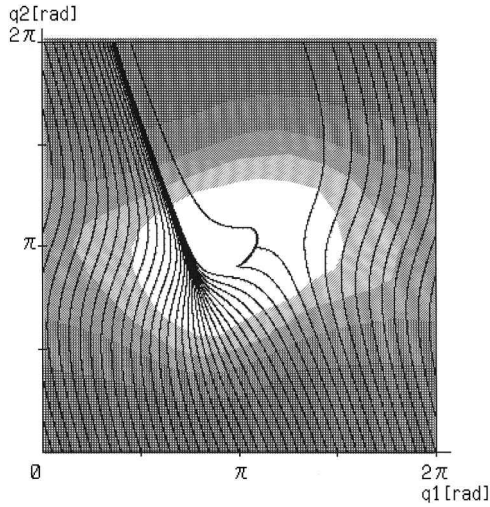§Professor; currently Professor, Osaka Institute of Technology, Hirakata 573-01, Japan. Member AIAA.

Fig. 1   Example of an EDM.

Minimum-Disturbance Path Planning

The purpose of the path planning is to reduce disturbances to the spacecraft attitude caused by the manipulator motion.[5] We compare two different algorithms for the manipulator path planning.

Algorithm 1

This algorithm determines the direction of joint movements that coincides with the direction to the desired terminal joint angles at each step.

1) Give the initial and desired positions of the end effector h^i and h^d, respectively.

2) Calculate the initial and desired terminal joint angles q^i and q^d, respectively.

3) Determine the vector of joint movements at the kth step δq^k to be in the direction of $q^d - q^k$, where q^d realizes h^d at the present attitude angle of the spacecraft χ^k.

4) Update the attitude angle and joint angles.

5) Compute the position vector of the end effector at the $(k+1)$th step h^{k+1} for χ^{k+1} and q^{k+1}.

6) If $|\Delta h^{k+1}| = |h^d - h^{k+1}| < \varepsilon$, terminate the maneuver. If not, repeat from step 3.

Algorithm 2

Algorithm 2 is a method of path planning that reduces the disturbances caused by joint movements. This algorithm differs from Algorithm 1 in step 3, where two directions of joint movements for each small step are taken into consideration. One of them, δq^a, is to realize the terminal joint angles, and the other, δq^b, is to reduce disturbances to the spacecraft attitude. The vector of total joint movements is determined as a weighted sum of these two vectors of joint movements, where the weighting depends on the magnitude of the disturbance caused by the joint movements. If the magnitude of disturbances is large, the joint movement is determined to reduce the disturbance, whereas if the magnitude of disturbances is small, it is determined to be nearly in the direction of the desired terminal joint angles. Step 3 of Algorithm 1 is revised as follows.

3-1) Determine δq_k^a as δq^k.

3-2) Determine δq_k^b for the attitude angle $\delta \chi_d^k = \chi^k - \chi^d$ to be corrected, where χ^d is the desired attitude of the spacecraft and χ^k is the attitude of the spacecraft at the kth step.

3-3) The vector of actual joint movements δq^k is determined at each step as follows:

$$\delta q^k = t \delta q^a + (1 - t) \delta q^b$$

where

$$t = \frac{n}{m+n}, \qquad m = \frac{|\delta \chi_k^a|}{\delta \chi^s}, \qquad n = \frac{\delta \chi^s}{|\delta \chi_k^a|} + \frac{\beta}{\Delta h}$$

and $\delta \chi_k^a$ is the magnitude of the disturbance caused by δq^k, $\delta \chi^s$ is the standard value of disturbances, Δh is the distance between the present position of the end effector and the desired position, and β is a real number.

Numerical Example

The specific mass and length parameters used in the simulation are as follows:

$$\text{mass } M_0 : M_1 : M_2 = 20.0 : 1.0 : 1.0$$

$$\text{length } l_0 : l_1 : l_2 = 1.0 : 1.0 : 1.0$$

The initial attitude of the spacecraft and initial and terminal positions of the end effector are given as

$$\chi^i = 0.0, \qquad h^i = (1.5, \ 1.5)^T, \qquad h^d = (0.4, \ 0.4)^T$$

Simulation results for the problem are presented in Figs. 2–4. The parameters used for the algorithms are chosen as

$$\alpha = 0.001 \text{ [rad]}, \qquad \beta = 0.5, \qquad \varepsilon = 0.001$$

Algorithm 2 reduces the attitude disturbances, as shown in Fig. 4. The attitude errors at the final stage of the maneuver are due to
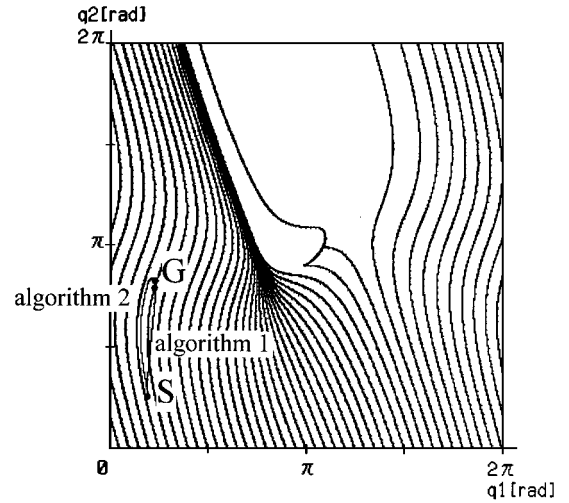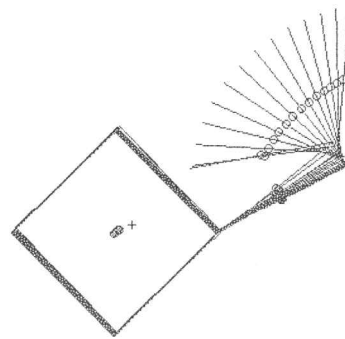

Fig. 2   Results of path planning on EDM.

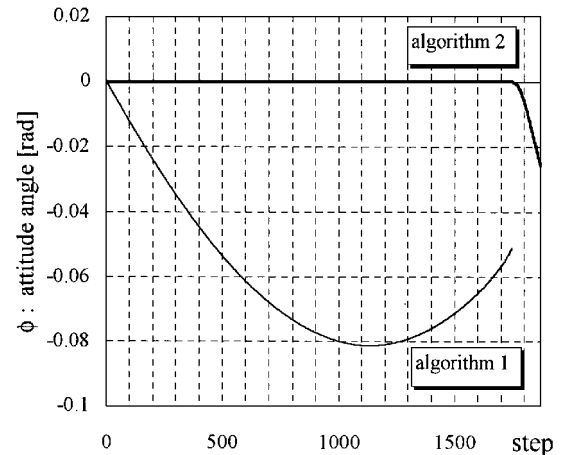**Fig. 3   Motion of the system with Algorithm 2.**

Fig. 4   Sequence of spacecraft attitude angles.

large weighting to the direction of joint movements for realizing the desired terminal conditions.

Conclusion

This Note proposes a method of path planning for space manipulators that reduces disturbances to the spacecraft attitude. The proposed method uses the EDM for planning the manipulator path in the joint space. The method sequentially determines the direction of small steps of joint movements that compromises the biobjectives of minimizing the disturbance to the spacecraft attitude and realizing the terminal end effector position. Numerical simulations have been made for a space robot with a two-link manipulator. The results of the simulations show the feasibility of the present path planning algorithm.

References

[1]Lindberg, R., Longman, R., and Zedd, M., "Kinematic and Dynamic Properties of an Elbow Manipulator Mounted on a Satellite," *Space Robotics: Dynamics and Control*, Kluwer Academic, Norwell, MA, 1993, pp. 1–25.

[2]Yamada, K., "Attitude Control of Space Robot by Arm Motion," *Journal of Guidance, Control, and Dynamics*, Vol. 17, No. 5, 1994, pp. 1050–1054.

[3]Vafa, Z., and Dubowsky, S., "On the Dynamics of Space Manipulators Using the Virtual Manipulator, with Applications to Path Planning," *Journal of the Astronautical Sciences*, Vol. 38, No. 4, 1990, pp. 441–472.

[4]Torres, M. A., and Dubowsky, S., "Minimizing Spacecraft Attitude Disturbances in Space Manipulator Systems," *Journal of Guidance, Control, and Dynamics*, Vol. 15, No. 4, 1992, pp. 1010–1017.

[5]Okubo, H., Nagano, N., Komatsu, N., and Tsumura, T., "Path Planning for Space Manipulators Using Enhanced Disturbance Map," *Proceedings of the AIAA Guidance, Navigation, and Control Conference* (Baltimore, MD), AIAA, Washington, DC, 1995, pp. 1510–1517.

Experimental Comparison of Robust $\mathcal{H}_2$ Control Techniques for Uncertain Structural Systems

Simon C. O. Grocott,* Jonathan P. How,†
and David W. Miller‡
*Massachusetts Institute of Technology,
Cambridge, Massachusetts 02139*

I. Introduction

INCREASING performance specifications require that many future spacecraft use active structural control to meet payload pointing performance specifications. The Middeck Active Control Experiment (MACE) was developed to investigate the issues associated with developing controllers for on-orbit operations, based on ground testing. The change from 1-g ground tests to 0-g experimentation introduces uncertainty in the fidelity of ground-based models; thus, robust control techniques must be used in the design of compensators.

This Note uses experimental results from MACE ground tests to present a comparison of sensitivity-weighted linear quadratic Gaussian (SWLQG),[1] maximum entropy (ME),[2,3] and multiple model (MM)[4] control with $\mathcal{H}_2$ optimal LQG,[5] looking particularly at the robustness/performance tradeoff.

II. $\mathcal{H}_2$ Control Techniques

Common to each of the control techniques is the system dynamics

$$\dot{x} = Ax + B_w w + B_u u$$

$$z = C_z x + D_{zw} w + D_{zu} u \qquad (1)$$

$$y = C_y x + D_{yw} w + D_{yu} u$$

which are controlled through a dynamic compensator of the form

$$\dot{x}_c = A_c x_c + B_c y, \qquad u = C_c x_c \qquad (2)$$

where w is a vector of uncorrelated white-noise disturbances with unit intensity, u is the control input vector, z is the performance vector, and y is the measurement vector.

Optimal $\mathcal{H}_2$ control (LQG)[5] minimizes the $\mathcal{H}_2$ norm (from w to z) of this system, or equivalently the cost functional

$$J = \lim_{t \to \infty} \mathbb{E}\{z^T z\} = \lim_{t \to \infty} \mathbb{E}\left\{ x^T R_{xx} x + 2x^T R_{xu} u + u^T R_{uu} u \right\} \quad (3)$$

For this Note, the noise (V_{xx}, V_{xy}, V_{yy}) and performance weights (R_{xx}, R_{xu}, R_{uu}) are completely defined by the actual disturbance inputs (w) and performance variables (z) so that

$$V = \begin{bmatrix} V_{xx} & V_{xy} \\ V_{xy}^T & V_{yy} \end{bmatrix} = \begin{bmatrix} B_w \\ D_{yw} \end{bmatrix} \begin{bmatrix} B_w^T & D_{yw}^T \end{bmatrix} \geq 0, \qquad V_{yy} > 0 \quad (4)$$

and

$$R = \begin{bmatrix} R_{xx} & R_{xu} \\ R_{xu}^T & R_{uu} \end{bmatrix} = \begin{bmatrix} C_z^T \\ D_{zu}^T \end{bmatrix} [C_z \quad D_{zu}] \geq 0, \qquad R_{uu} > 0 \quad (5)$$

This definition is restrictive but results in optimal $\mathcal{H}_2$ controllers for the system in Eq. 1.

The maximum entropy[2,3] approach minimizes the cost functional [Eq. (3)] but uses a multiplicative white-noise model of parametric uncertainty in the dynamics. The maximum entropy equations of Collins et al.[3] are designed for handling uncertainty in natural frequencies of flexible structures and are used herein. The equations provide weightings (δ_i) for each mode that is considered uncertain.

The multiple model technique minimizes a weighted average of the $\mathcal{H}_2$ norms of a discrete set of models.[4] Robustness is added by selecting a set of models that have different values for uncertain parameters. In this Note, the number of models is always three: one is the nominal model, and the other two have positive and negative shifts, respectively, of each of the uncertain modes. The solution is obtained through a quasi-Newton optimization.

Finally, the SWLQG technique requires some elaboration because no complete reference is available. SWLQG is essentially an LQG problem that is suboptimal for the system in Eq. (1) but is more robust than the optimal. It provides a formal method for choosing the weights (R and V) to provide good $\mathcal{H}_2$ performance for the system with greater robustness.

Ignoring for a moment the noise input w in Eq. (1), SWLQR[1] optimizes the standard LQR cost functional with an additional quadratic term in the sensitivity states of the system

$$J = \lim_{T \to \infty} \int_0^T x^T R_{xx} x + \sum_{i=1}^{n_\alpha} \frac{\partial x^T}{\partial \alpha_i} R_{\alpha \alpha_i} \frac{\partial x}{\partial \alpha_i}$$

$$+ 2x^T R_{xu} u + u^T R_{uu} u \, dt \qquad (6)$$

where $\partial x / \partial \alpha_i$ is the sensitivity state vector and is obtained by differentiating Eq. (1) to yield

$$\frac{\partial \dot{x}}{\partial \alpha_i} = A \frac{\partial x}{\partial \alpha_i} + \frac{\partial A}{\partial \alpha_i} x + B_u \frac{\partial u}{\partial \alpha_i} + \frac{\partial B_u}{\partial \alpha_i} u \qquad (7)$$

The solution of this problem is not finite dimensional because of the presence of the $\partial u / \partial \alpha_i$ term. However, several methods[6] exist for approximating $\partial u / \partial \alpha_i$, with the simplest being to assume that $\partial u / \partial \alpha_i$ is small and neglect its contribution.